Effects of the Surface Roughness on Sliding Angles of Water Droplets on Superhydrophobic Surfaces

Masashi Miwa,† Akira Nakajima,† Akira Fujishima,‡ Kazuhito Hashimoto,*,† and Toshiya Watanabe*,†

Research Center for Advanced Science and Technology, The University of Tokyo, 4-6-1 Komaba, Meguro-ku, Tokyo 153-8904, Japan, and Department of Applied Chemistry, School of Engineering, The University of Tokyo, 7-3-1 Hongo, Bunkyo-ku, Tokyo 113-8656, Japan

Received December 20, 1999. In Final Form: March 22, 2000

Various superhydrophobic films having different surface roughnesses were prepared, and the relationships between the sliding angle, the contact angle, and the surface structure were investigated. In the highly hydrophobic region, the sliding angles of water droplets decreased with increasing contact angles. Microstructural observation revealed that surface structures that can trap air are important for the preparation of low-sliding-angle surfaces. We have also derived an equation that describes the relationship between sliding angles and contact angles on superhydrophobic surfaces with roughness. The results calculated on the basis of this equation agreed well with the experimental ones. Moreover, we have successfully prepared a transparent superhydrophobic film whose sliding angle is ∼1° for a 7 mg water droplet. On this film, there was almost no resistance to the sliding of water droplets. The film obtained satisfies the requirements of superhydrophobicity, transparency, and a low water sliding angle.

Introduction

Wettability is one of the important properties of solid surfaces from both fundamental and practical aspects. Among various factors, surface energy and surface roughness are the dominant factors for the wettability. When the surface energy is lowered, the hydrophobicity is enhanced. However, even a material with the lowest surface energy (6.7 mJ/m^2 for a surface with regularly aligned closest-hexagonal-packed $-CF_3$ groups) gives a water contact angle of only around 120°.[1] For higher hydrophobicity, providing a proper surface roughness is required.[2] In fact, surfaces with a water contact angle of more than 150° were developed by introducing proper roughness on materials having low surface energies.[3−23]

While the contact angle of water has been commonly used as a criterion for the evaluation of hydrophobicity of the surface, this alone is insufficient for the evaluation of the sliding properties of water droplets on surfaces.[21,23−26] A surface with a high contact angle does not always show a low sliding angle, which is defined as the critical angle where a water droplet with a certain weight begins to slide down the inclined plate. For example, Murase et al. demonstrated that a fluoropolymer with a water contact angle of 117° shows a higher sliding angle than a poly(dimethylsiloxane) with a water contact angle of 102°.[24−26] They have proposed that this phenomenon is due to a negative excess entropy caused by the rigidity of fluoropolymer segments and the enhancement of an icelike molecular arrangement in water.[25,26] Therefore, when we discuss hydrophobicity, the sliding property of water droplets should be evaluated separately from the contact angle.

Bikerman investigated sliding angles on stainless steel plates with different finishes, having the contact angles around 90°, and proposed that the surface roughness provides resistance for the sliding of water droplets.[27] Johnson and Dettre theoretically simulated the effect of the surface roughness on the difference between the

* Corresponding authors. E-mail: kazuhito@fchem.chem.t.u-tokyo.ac.jp, watanabe@fchem.chem.t.u-tokyo.ac.jp.
† Research Center for Advanced Science and Technology.
‡ Department of Applied Chemistry.

(1) Nishino, T.; Meguro, M.; Nakamae, K.; Matsushita, M.; Ueda, Y. *Langmuir* **1999**, *15*, 4321.
(2) Wenzel, R. N. *J. Phys. Colloid Chem.* **1949**, *53*, 1466.
(3) Dettre, R. H.; Johnson, R. R., Jr. *Adv. Chem. Ser.* **1963**, *43*, 136.
(4) Washo, B. D. *Org. Coat. Appl. Polym. Sci. Proc.* **1982**, *47*, 69.
(5) Morra, M.; Occhiello, E.; Garbassi, F. *Langmuir* **1989**, *5*, 872.
(6) Kunigi, Y.; Nonaku, T.; Chong, Y.-B.; Watanabe, N. *J. Electroanal. Chem.* **1993**, *353*, 209.
(7) Ogawa, N.; Soga, M.; Takada, Y.; Nakayama, I. *Jpn. J. Appl. Phys.* **1993**, *32*, L614.
(8) Onda, T.; Shibuichi, S.; Satoh, N.; Tsujii, K. *Langmuir* **1996**, *12*, 2125.
(9) Yamauchi, G.; Miller, J. D.; Saito, H.; Takai, K.; Ueda, T.; Takazawa, H.; Yamamoto, H.; Nishi, S. *Colloids Surf., A* **1996**, *116*, 125.
(10) Shibuichi, S.; Onda, T.; Satoh, N.; Tsujii, K. *J. Phys. Chem.* **1996**, *100*, 19512.
(11) Saiki, Y.; Nakao, M.; Ono, M. *Kogyo-Zairyo* **1996**, *44* (8), 52 (in Japanese).
(12) Tsujii, T.; Yamamoto, T.; Onda, T.; Shibuichi, S. *Angew. Chem., Int. Ed. Engl.* **1997**, *36*, 1011.
(13) Tadanaga, K.; Katata, N.; Minami, T. *J. Am. Ceram. Soc.* **1997**, *80*, 1040.
(14) Hozumi, A.; Takai, O. *Thin Solid Films* **1997**, *303*, 222.
(15) Takai, O.; Hozumi, A.; Inoue, Y.; Komori, T. *Bull. Mater. Sci.* **1997**, *20*, 817.
(16) Tadanaga, K.; Katata, N.; Minami, T. *J. Am. Ceram. Soc.* **1997**, *80*, 3213.
(17) Tokuumi, A.; Hiromatsu, K.; Kumai, S.; Mihara, H. *Toso-to-Toryo* **1998**, *571*, 37 (in Japanese).
(18) Sasaki, H.; Shouji, M. *Chem. Lett.* **1998**, 293.
(19) Shibuichi, S.; Yamamoto, T.; Onda, T.; Tsujii, K. *J. Colloid Interface Sci.* **1998**, *208*, 287.
(20) Hozumi, A.; Takai, O. *Thin Solid Films* **1998**, *332*, 54.
(21) Chen, W.; Fadeev, A. Y.; Hsieh, M. C.; Öner, D.; Youngblood, J.; McCarthy, T. J. *Langmuir* **1999**, *15*, 3395.
(22) Nakajima, A.; Fujishima, A.; Hashimoto, K.; Watanabe, T. *Adv. Mater.*, **1999**, *11*, 1365.
(23) Youngblood, J. P.; McCarthy, T. J. *Macromolecules* **1999**, *32*, 6800.
(24) Murase, H.; Nanishi, K.; Kogure, H.; Fujibayashi, T.; Tamura, K.; Haruta, N. *J. Appl. Polym. Sci.* **1994**, *54*, 2051.
(25) Murase, H.; Fujibayashi, T. *Prog. Org. Coat.* **1997**, *31*, 97.
(26) Murase, H. *Proceedings of the Fifth Interface Meeting of the Science Council of Japan*; Tokyo, 1998 (in Japanese).
(27) Bikerman, J. J. *J. Colloid Sci.* **1950**, *5*, 349.

10.1021/la991660o CCC: $19.00
Published on Web 05/27/2000

advancing and receding contact angles,[28] which is termed contact angle hysteresis and is commonly used as a criterion for the sliding properties. They suggested that the hysteresis on hydrophobic surfaces increases with increasing surface roughness in the low-roughness region but decreases drastically when the roughness becomes large and the composite configuration, in which the liquid does not penetrate into the troughs, is energetically preferred.

Furmidge derived an equation describing the relationship between the hysteresis and the sliding angle[29]

$$(mg \sin \alpha)/w = \gamma_{LV}(\cos \theta_R - \cos \theta_A) \quad (1)$$

where α is the sliding angle, m is the weight of the water droplet, w is the width of the droplet, γ_{LV} is free energy of the liquid at the liquid−gas interface, and θ_R and θ_A are the receding and advancing contact angles. As this equation indicates, surfaces with the same hysteresis values do not always show the same water sliding angles because the m/w value varies with different contact angles. Therefore, to evaluate the sliding properties of surfaces with different contact angles, the direct comparison of the sliding angle itself is preferable.

So far, there have been few studies on the relationships between the sliding angle, the contact angle, and the microstructure of rough hydrophobic surfaces, and a comprehensive understanding of the sliding properties on superhydrophobic surfaces is still insufficient. In the present study, we have prepared superhydrophobic surfaces with various roughnesses and have investigated the relationships between the sliding angle, the contact angle, and the surface structure. This work builds upon our recently published work,[22] which focused on the preparation of transparent superhydrophobic boehmite and silica films, prepared by sublimation of aluminum acetylacetonate. We have also now been able to prepare a transparent superhydrophobic film with sliding angle about 1°, which had not previously been possible. On this type of film, we report herein the observation of a constant acceleration motion of water droplets. Moreover, we discuss the effect of the surface roughness on sliding angles on the basis of a new theoretical model.

Background

Contact Angle on a Rough Solid Surface. The contact angle θ of a liquid droplet on a flat solid surface is given by Young's equation, eq 2.

$$\cos \theta = \frac{\gamma_{SV} - \gamma_{SL}}{\gamma_{LV}} \quad (2)$$

where γ_{SL}, γ_{SV}, and γ_{LV} are the interfacial free energy per unit area of the solid−liquid, solid−gas, and liquid−gas interfaces, respectively. However, this equation can be applied only to a flat surface and not to a rough one. Thus, several models describing the contact angle at a rough solid surface have been proposed so far. Wenzel proposed a theoretical model describing the contact angle θ' at a rough surface.[2] He modified Young's equation as follows

$$\cos \theta' = \frac{r(\gamma_{SV} - \gamma_{SL})}{\gamma_{LV}} = r \cos \theta \quad (3)$$

where r is a roughness factor, which is defined as the ratio of the actual area of a rough surface to the geometric projected area. This equation indicates that the surface roughness enhances the hydrophilicity of hydrophilic surfaces and also enhances the hydrophobicity of hydrophobic ones because r is always larger than 1.

Cassie proposed an equation describing the contact angle θ' at a heterogeneous surface composed of two different materials. When a unit area of the surface has a surface area fraction f_1 with a contact angle θ_1 and an area fraction f_2 with a contact angle θ_2, the contact angle on the surface can be expressed by the following equation:[30]

$$\cos \theta' = f_1 \cos \theta_1 + f_2 \cos \theta_2 \quad (4)$$

When f_2 represents the area fraction of trapped air, eq 4 can be modified as follows

$$\cos \theta' = f \cos \theta + (1 - f)\cos 180° = f \cos \theta + f - 1 \quad (5)$$

where f is the remaining area fraction, i.e., liquid−solid interface. This equation can also be used for rough hydrophobic surfaces trapping air in the hollows of the rough surface.

Sliding Angle. Wolfram et al. have proposed an empirical equation describing the sliding angle of droplets on smooth surfaces of various materials[31,32]

$$\sin \alpha = k\frac{2r\pi}{mg} \quad (6)$$

where α is the sliding angle, r is the radius of the contact circle, m is the weight of the droplet, g is the gravitational acceleration, and k is a proportionality constant.

Murase et al. modified this equation to describe the relationship between the sliding angle and the contact angle by using the following equations[26]

$$r = R \sin \theta \quad (7)$$

$$^3/_4 \pi R'^3 \rho g = mg \quad (8)$$

$$R' = \left\{\frac{1}{4}(2 - 3 \cos \theta + \cos^3 \theta)\right\}^{1/3} R \quad (9)$$

where ρ is the specific weight of water and R' and R are the radii of the droplet with a mass m before and after attachment to the surface, respectively. Substitution of eqs 7, 8, and 9 in eq 6 leads to eq 10.

$$k = \left\{\frac{9m^2(2 - 3 \cos \theta + \cos^3 \theta)}{\pi^2}\right\}^{1/3} \frac{\sin \alpha \, (g\rho^{1/3})}{6 \sin \theta} \quad (10)$$

By using this equation, the constant k for any flat surface can be obtained from measurable values, α, θ, and m. Murase pointed out that k is related to the interaction energy between solid and liquid.

Experimental Section

Materials. Hydrophobic surfaces with various surface roughnesses were prepared by use of a method utilizing the sublimation of aluminum acetylacetonate (AACA, $Al(C_5H_7O_2)_3$).[22] The surface structures are easily varied by changing the composition of the starting materials by this method.

(28) Johnson, R. E., Jr.; Dettre, R. H. *Adv. Chem. Ser.* **1963**, *43*, 112.
(29) Furmidge, C. G. L. *J. Colloid Sci.* **1962**, *17*, 309.
(30) Cassie, A. B. D. *Discuss. Faraday Soc.* **1948**, *3*, 11.
(31) Buzágh, A.; Wolfram, E. *Kolloid Z.* **1956**, *149*, 125.
(32) Wolfram, E.; Faust, R. *Wetting, Spreading, and Adhesion*; Padday, J. F., Ed.; Academic Press: London, 1978; Chapter 10.

A commercial boehmite powder (AlOOH, DISPAL 18N4, Condea Chemie, Germany) and reagent-grade AACA (Tokyo Kasei Co., Japan) were mixed with ethanol (Wako Junyaku Co., Japan). The weight ratio of AACA to ethanol was fixed to 0.0366, and that of boehmite to ethanol was varied from 0.0008 to 0.0096 to control the roughness of the surface. The suspensions were sonicated for 20 min, resulting in the dissolution of AACA into ethanol.

The sonicated suspensions were coated on Pyrex glass plates (1 mm in thickness) by spin-coating at 1000 rpm for 10 s. The coated glass plates were calcined at 500 °C for 20 s. White smoke was generated, and the boehmite films were roughened by the sublimation of AACA during calcination. These coating and calcination procedures were repeated five times to coat the glass plates completely with boehmite.

Heptadecafluorodecyltrimethoxysilane ($CF_3(CF_2)_7CH_2CH_2Si(OCH_3)_3$, TSL8233, Toshiba Silicone Co., Japan, hereafter referred to as FAS-17) was used as a water-repellent agent. A methanol solution of FAS-17 was hydrolyzed by the addition of a 3-fold molar excess of water at room temperature. This solution was evaporated at 250 °C and coated on the plates, resulting in a hydrophobic film surface. The same coating process was also carried out on a flat Pyrex glass plate for comparison.

Evaluation. The sessile drop method was used for contact angle measurements with a commercial contact angle meter (CA-X, Kyowa Interface Science, Japan). The water droplet size used for the measurements was 3 mg. The contact angles were measured at five different points for each sample. The contact angle value obtained by this method is strictly one of the many thermodynamically allowed metastable states, experimentally indistinguishable from the actual equilibrium contact angle. However, we use this value as the experimental contact angle in this paper. The sliding angles of water droplets were measured by a commercial sliding angle measurement system (SA-11, Kyowa). The water droplet size for these measurements was varied from 7 to 40 mg. The surface was blown with ionized air to eliminate static electricity on the surface before each measurement. Sequence photographs of the sliding behavior of the water droplets on inclined surfaces were taken every 33 ms with an automatic contact angle meter (CA-V, Kyowa) equipped with a computer-controlled camera. Microstructure was observed by scanning electron microscopy (SEM, S-4200, Hitachi Co., Japan) and atomic force microscopy (AFM, SPA300, Seiko Instruments Inc., Japan). The AFM measurements were performed in the noncontact mode, and microfabricated silicon cantilevers with a bending spring constant of 1.6 N/m and a resonance frequency of 27 kHz (SI-DF3-A, Seiko Instruments Inc.) were used for imaging in air with a 20 μm scanner. The scan rate was 0.5 Hz. The surface topographical images of the prepared films obtained by AFM were treated by using the SPI3700 probe station AFM software, version 1.35 (Seiko Instruments Inc.). All images were processed using procedures for plane-fit and flatten. Average roughness (R_a) of the prepared film surface is calculated from the following equation[33]

$$R_a = \frac{1}{S_0}\int\int |Z(X, Y)| \mathrm{d}X \mathrm{d}Y \qquad (11)$$

where $Z(X, Y)$ is the elevation for a given point, Z_0 is the average of the elevation within the given area, and S_0 is the projected area of the given area. The surface area ratio, that is, the difference between the actual surface area and the geometrical surface area, was also calculated from the topographical images. Transmittance of visible light was evaluated with an UV−vis−near-IR scanning spectrophotometer (UV-3100PC, Shimadzu Co., Japan).

Results

Surface Structures. Parts a−d of Figure 1 show SEM micrographs of the prepared film surfaces with boehmite−ethanol ratios of 0.0084, 0.0036, 0.0024, and 0.0008, respectively. These micrographs reveal that the packing of boehmite powder in the film becomes looser as the boehmite−ethanol ratio decreases. AFM images of cross sections of the same surfaces are shown in Figure 2. All of the surfaces consist of assemblies of needlelike structures, whose pitch is much less than 1 μm. As the boehmite−ethanol ratio decreases, the structure becomes sharper. However, the heights of the needles are highest for the film with the boehmite−ethanol ratio of 0.0024. The 3D image of this surface is shown in Figure 3. The average roughness of the surface is calculated to be 59 nm from this topographical image, and the surface area ratio is calculated to be 1.82. The SEM observation of a section of this sample revealed that the film thickness of the sample was 200−300 nm.

Contact Angles and Sliding Angles. The flat glass plate coated with FAS-17 showed a water contact angle of 105.4° (average) ± 0.8° (standard deviation). The contact angles on the prepared surfaces are plotted against the boehmite−ethanol ratio in Figure 4a. When the boehmite−ethanol ratio decreases, the contact angle first increases gradually from 147.1° ± 0.9° to 160.9° ± 0.7°, becomes almost constant, and then starts decreasing sharply.

Figure 5 shows the variation of sliding angles with the weights of the water droplets for a flat glass plate coated with FAS-17. The sliding angle increases as the weight of the droplet decreases, and droplets below 12 mg do not slide, even if the plate is vertical. The constant k in eq 10 was calculated from the experimental data in Figure 5 to be 12.49 ± 0.15 mJ/m^2. The theoretical line fitted by use of this k value coincided well with the experimental data points. Figure 4b shows the variation of the sliding angle for a 7 mg water droplet with the boehmite−ethanol ratio. The sliding angle gradually decreases with decreasing ratio and shows an abrupt minimum in the region between 0.0012 and 0.0030. The lowest sliding angle for a 7 mg water droplet was less than 1°, which was observed on the films with boehmite−ethanol ratios of 0.0016 and 0.0024. Figure 6 shows the sliding behavior of a water droplet on a 1° tilted surface with the boehmite−ethanol ratio of 0.0024. From these sequence photographs, we estimated the sliding rate as a function of time, as shown in Figure 7. A straight line was fitted to the points by least-squares fitting. This figure indicates that once the droplet starts moving, it follows a constant accelerated motion, with an acceleration of 0.20 m/s^2. This value is nearly equal to g sin 1° (0.17 m/s^2), indicating that there was almost no resistance for the sliding of water droplets on this surface. This measurement was repeated five times using the different samples of the same boehmite−ethanol ratio. While the acceleration rate on each sample varied because of the accuracy of the tilting angle control, which is of the order of 1°, a constant-acceleration motion of water droplets was reproduced on each sample, so that the correlation factor was 0.9966 ± 0.0018. Transmittance of visible light for the film with the boehmite−ethanol ratio of 0.0024 is shown in Figure 8. The surface roughness of this film is small enough to inhibit light scattering, and thus the transmittance in the visible range is almost the same as that of Pyrex glass.

Discussion

Relationship between the Sliding Angle and the Surface Structure. The experimental results show that both the contact angle and the sliding angle are strongly affected by the surface structure. The surfaces formed with taller needles show higher contact angles and lower sliding angles. In Figure 9, the sliding angles are plotted

(33) *SPA300 scanning probe microscope operation manual*; Seiko Instruments Inc.: Chiba, Japan, 1994.

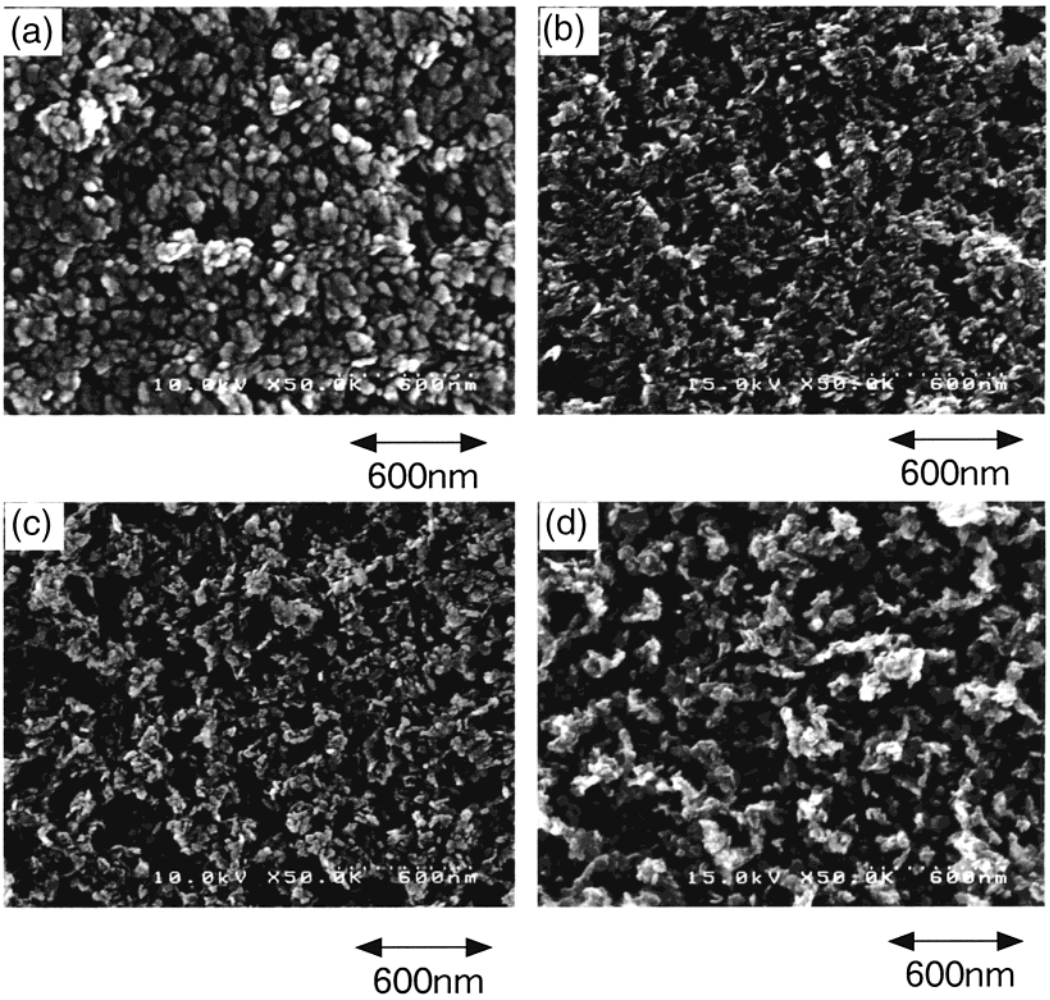

Figure 1. SEM micrographs of the prepared film surfaces with boehmite−ethanol ratio (a) 0.0084, (b) 0.0036, (c) 0.0024, and (d) 0.0008.

against the contact angles. In the highly hydrophobic region investigated in this study, the sliding angle decreases drastically for larger contact angles. This result is consistent with that of Johnson and Dettre on the contact angle hysteresis in the highly hydrophobic region.[28] They proposed that this is due to the transition from a noncomposite (i.e., completely liquid−solid interface) to a composite surface (including trapped air), which is expressed by Cassie's equation.

All of these results suggest that the air trapped in the surface structure plays an important role for a surface with a low sliding angle. The needlelike structure may serve as a means of trapping sufficient air for low sliding angles to be exhibited. Surface structures such as that shown in Figure 2c have projections with proper heights at proper intervals to trap sufficient air in the structure. Conversely, structures such as that shown in Figure 2a have projections that are too low to trap sufficient air.

Model for Sliding Angles on Rough Surfaces. On the basis of the obtained results, we propose a model describing sliding angles on rough surfaces. We assume that the surface has a series of uniform needles, as illustrated in Figure 10. The contact angle on this model surface is described by combining eq 3 with eq 5 as follows

$$\cos \theta' = rf \cos \theta + f - 1 \qquad (12)$$

where θ' is the equilibrium contact angle on a rough surface, θ is the equilibrium contact angle on a flat surface, r is the ratio of the side area to the bottom area of the needle, which is represented by a/b in Figure 10, and f is the projected area fraction of the surface contacted with water, which is represented in one dimension to be $\Sigma b/(\Sigma b + \Sigma c)$ in Figure 10. In this equation, rf represents the ratio of the substrate−water interface area to the projected surface area. Using this equation, we now derive an equation representing the relation between sliding angle and contact angle on a rough surface.

Let us introduce the following assumptions to make this model simpler.

(1) The shapes of the tips of the needles are constant for all of the surfaces; that is, r has a constant value. The contact angle varies only with the fraction value f.

(2) The interaction energy between water and substrate is proportional to the true contact area, which is rf times as large as the apparent contact area. Therefore, the constant related to the interaction energy k in eq 10 is assumed to be rf times as great as that for the flat surface.

(3) Experimental contact angles are equal to equilibrium contact angles.

Introduction of assumption 2 to eq 10 gives the next expression for a rough surface.

$$\sin \alpha = \frac{2rfk \sin \theta'}{g}\left\{\frac{3\pi^2}{m^2 \rho(2 - 3\cos \theta' + \cos^3 \theta')}\right\}^{1/3} \qquad (13)$$

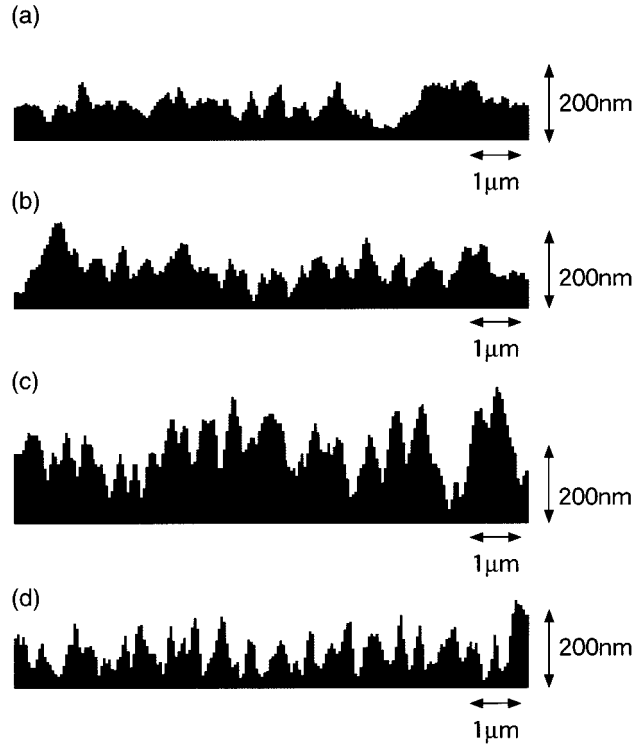

Figure 2. AFM images of cross sections of the prepared film surfaces with boehmite−ethanol ratio (a) 0.0084, (b) 0.0036, (c) 0.0024, and (d) 0.0008.

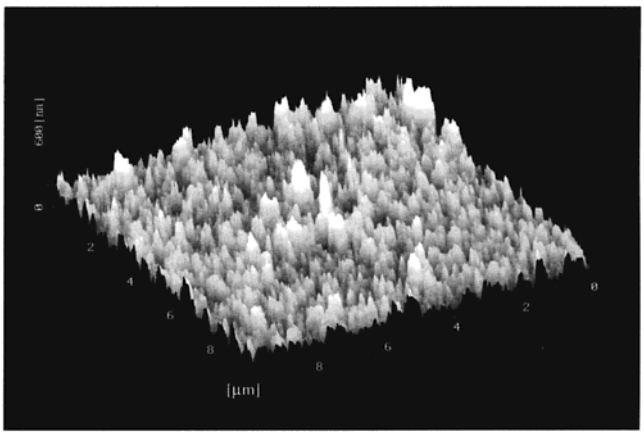

Figure 3. AFM 3D image of the prepared film surface with the boehmite−ethanol ratio of 0.0024.

Substitution of eq 12 into eq 13 leads to eq 14.

$$\sin\alpha = \frac{2rk\sin\theta'(\cos\theta'+1)}{g(r\cos\theta+1)}\left\{\frac{3\pi^2}{m^2\rho(2-3\cos\theta'+\cos^3\theta')}\right\}^{1/3} \quad (14)$$

Now we have obtained an equation (eq 14) that describes the relationship between the contact angle θ' and the sliding angle α on a rough surface. The curves drawn in Figure 9 were calculated from this equation. For this calculation, we have used the experimentally determined contact angle θ (105.4°) and the constant k (12.49 mJ/m^2) for a smooth glass surface coated with FAS-17. The curve for Cassie's model was calculated by setting r to 1 in eq 14. That for Wenzel's model was obtained by eliminating r from eq 13 by substitution of eq 12, and by assuming $f = 1$ in the equation obtained. On the basis of these calculations, it is apparent that a low water sliding angle is attained from a superhydrophobic surface that obeys Cassie's model. In the contact angle region from 145° to 156°, experimental results are simulated with eq 14, with an r value of 2.4. When the contact angle was greater than 158°, however, the sliding angle turns out to be in good agreement with Cassie's model, showing that the assumption of constant r is not satisfied when the contact angle becomes very large. We propose that water droplets are actually riding only on the extreme top portions of the needles on the film with the boehmite−ethanol ratio of 0.0024. Because of the high air ratio at the interface between solid and water, the sliding resistance is drastically reduced, and a low water sliding angle is attained. Therefore, on the basis of eq 14, we conclude that a high trapped-air ratio and small r are indispensable for

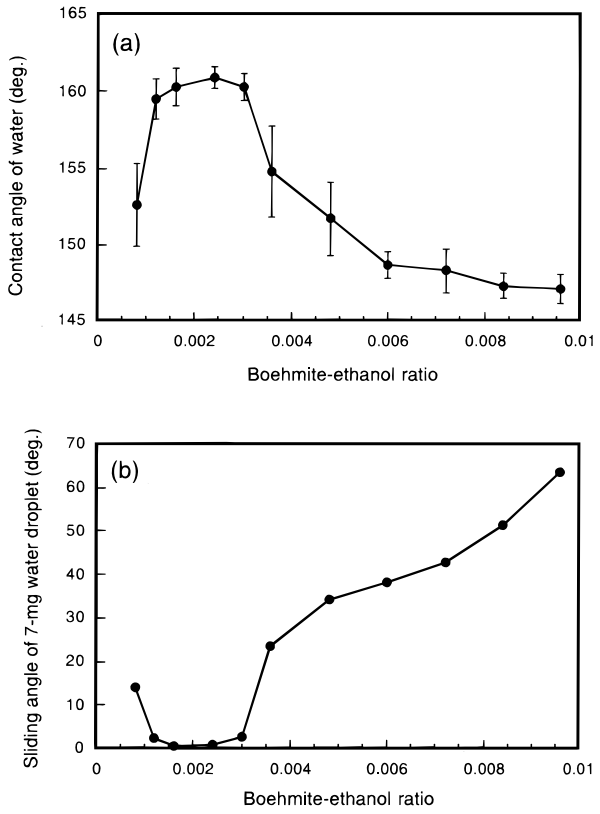

Figure 4. (a) Water contact angle on the surfaces plotted against the boehmite−ethanol ratio. (b) The dependence of the sliding angle of a 7 mg water droplet on the boehmite−ethanol ratio.

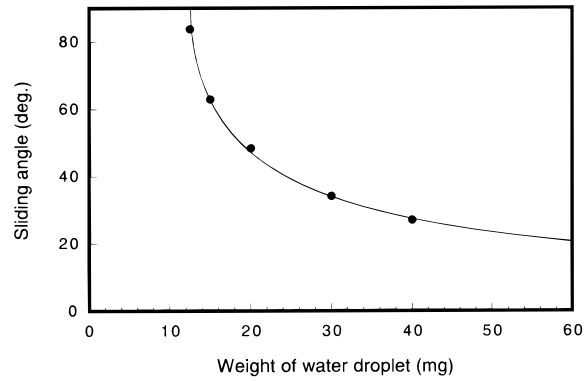

Figure 5. Variation of sliding angles with the weights of water droplets for a flat glass plate coated with FAS-17. The curve was calculated by use of eq 10.

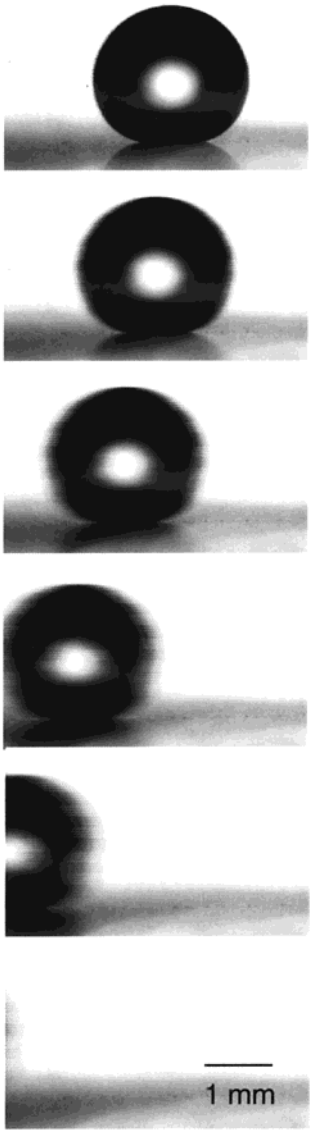

Figure 6. Sliding behavior of a water droplet on the prepared film (boehmite−ethanol ratio: 0.0024). (Drop weight, 7 mg; tilt angle of surface, 1°; high-speed photography with 33 ms/frame)

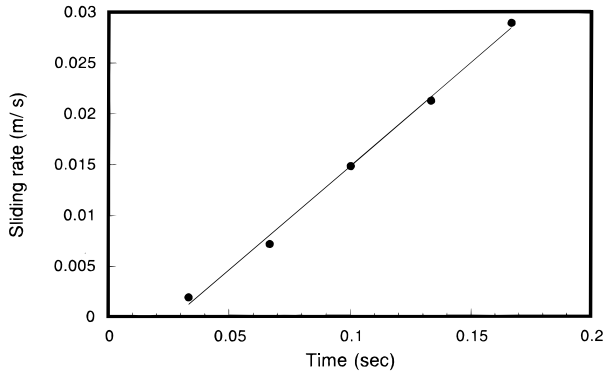

Figure 7. Variation of the sliding rate of a water droplet on the same film as shown in Figure 6 tilted at 1°.

excellent superhydrophobicity. Our film satisfies these conditions, and thus it exhibits extremely high water-repellency.

As far as we know, the sliding angle of ~1° for a 7 mg water droplet is the lowest value reported for solid surfaces. Moreover, this is the first report of the constant acceleration of water droplets on a superhydrophobic surface. We believe that the sliding rate of water droplets is another important criterion for the evaluation of hydrophobic surfaces.

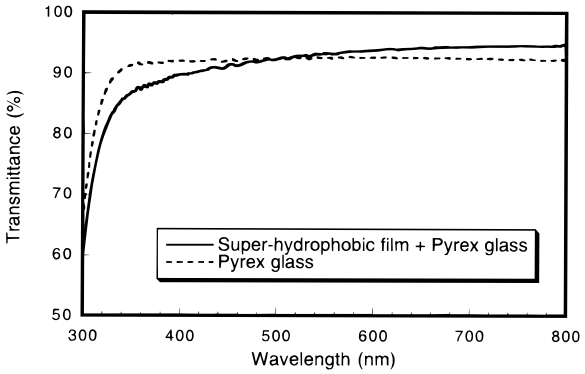

Figure 8. Transmittance of the same film as shown in Figure 6 in the visible wavelength region.

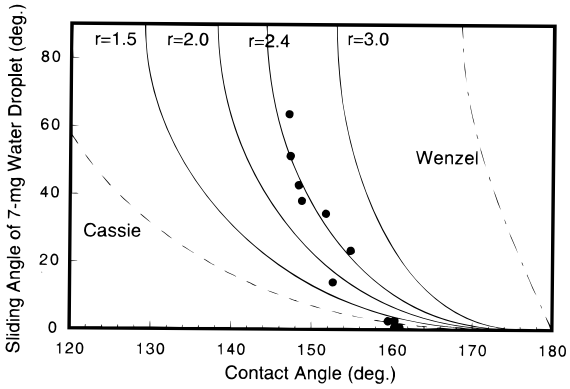

Figure 9. Dependence of the sliding angle on the contact angle: (−•−) curve obtained by use of Wenzel's equation; (- - -) curve obtained by use of Cassie's equation; (—) curves obtained by use of eq 14.

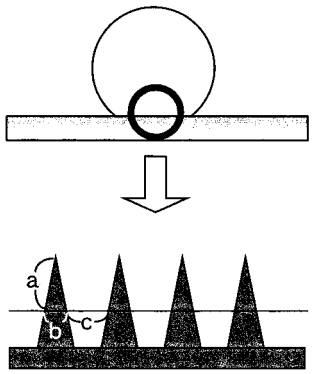

Figure 10. Schematic illustration of the surface model with a series of uniform needles.

Conclusions

In the present study, superhydrophobic surfaces with various roughnesses were prepared, and the sliding angles on the rough surfaces were evaluated. In the highly hydrophobic region, the sliding angles of water droplets decrease with increasing contact angle, which is considered to depend on the surface roughness. Microstructural observation revealed that surface structures that can trap air are important for the preparation of low-sliding-angle surfaces.

Assuming a surface model, we have for the first time proposed an equation that describes the relationship

between sliding angles and contact angles on superhydrophobic surfaces with roughness. The results calculated on the basis of this equation agree well with the experimental results.

By the optimization of the surface structure, we have successfully prepared a transparent superhydrophobic film whose sliding angle is ∼1° for a 7 mg water droplet. On this film, there was almost no resistance to the sliding of water droplets. This type of film satisfies the requirements of superhydrophobicity, transparency, and a low water sliding angle, and therefore it has great potential for practical applications.

Acknowledgment. We are grateful to Prof. D. A. Tryk for careful reading of the manuscript. Experimental supports by Kyowa Interface Science Co., Ltd. and Seiko Instruments Inc. are gratefully acknowledged. Financial support by a Grant-in-Aid for Scientific Research on Priority Areas, Electrochemistry of Ordered Interfaces, from the Ministry of Education, Science, Sports and Culture of Japan is gratefully acknowledged.

LA991660O